Hydrogen bond in 3-acetyl-4-hydroxycoumarin: X-ray diffraction study and quantum-chemical calculations

K. A. Lyssenko and M. Yu. Antipin*

A. N. Nesmeyanov Institute of Organoelement Compounds, Russian Academy of Sciences, 28 ul. Vavilova, 117813 Moscow, Russian Federation. Fax: +7 (095) 135 5085. E-mail: kostya@xrlab.ineos.ac.ru

The proton transfer and the character of the strong intramolecular O—H...O hydrogen bond (O...O 2.442 Å) in 3-acetyl-4-hydroxycoumarin were analyzed based on the results of X-ray diffraction study in the temperature range from 100 to 353 K and quantum-chemical B3LYP/6-31G(d,p) calculations. The barrier to proton transfer along the H-bond line is low (2 kcal mol^{-1}). However, no proton transfer was observed in the crystal at 100 K. Bader's topological analysis of the electron density distribution both in the crystal and in the isolated molecule demonstrated that the hydrogen bond corresponds to an intermediate type of interatomic interactions ($E(\mathbf{r}) < 0$, $\nabla^2\rho(\mathbf{r}) > 0$ at the critical point (3, −1)).

Key words: 3-acetyl-4-hydroxycoumarin, intramolecular hydrogen bond, proton transfer, electron density distribution, topological analysis of the electron density distribution, X-ray diffraction analysis, *ab initio* quantum-chemical calculations.

cis-Enols of β-diketones represent a known class of organic compounds with rather strong intramolecular hydrogen bonds (hereinafter, H-bonds). The low barriers to proton transfer (*e.g.*, 4.2 and 2.9 kcal mol^{-1} for malonaldehyde and acetylacetone, respectively[1]) allow one to attack the fundamental problems of theoretical chemistry, such as proton transfer[2,3] and the possibility of the formation of symmetrical four-electron three-center 4e,3c-hydrogen bonds,[4] in studies of the tautomeric keto-enol equilibrium. Detailed information on the nature of H-bonds can be obtained by different physicochemical methods (NMR and IR spectroscopy, neutron diffraction studies, X-ray diffraction analysis, and quantum-chemical calculations[5,6]).

High-resolution X-ray diffraction studies of systems containing hydrogen bonds are of particular interest because this method enables one not only to accurately determine the geometric parameters of the molecules and to analyze the character of thermal motion of the atoms, but also (which is more attractive) to study the nature of H-bonds by examining the electron density distribution function $\rho(\mathbf{r})$ in the crystal.[7]

One of modern approaches to the analysis of the experimental and theoretical $\rho(\mathbf{r})$ functions is based on the topological theory known as "Atoms in Molecules" (AM).[8] This theory allows one to unambiguously reveal the existence of a chemical bond between two atoms based on the critical points (CP) of the $\rho(\mathbf{r})$* function and to relate the topology of the electron density distribution to the local energy contributions and, hence, to elucidate the character of interatomic interactions.[8—10] The last-named possibility stems from the fact that the Laplacian of the electron density distribution function $\nabla^2\rho(\mathbf{r})$ appears in the local expression of the virial theorem:[9,10]

$$(\hbar^2/4m)\nabla^2\rho(\mathbf{r}) = 2G(\mathbf{r}) + V(\mathbf{r}), \qquad (1)$$

where $G(\mathbf{r})$ and $V(\mathbf{r})$ are the local densities of the kinetic and potential energies, respectively. Since, by definition, $G(\mathbf{r}) > 0$ and $V(\mathbf{r}) < 0$, not only does the sign of $\nabla^2\rho(\mathbf{r})$ signify the local accumulation or depletion of the $\rho(\mathbf{r})$ function at the point r, but it also indicates which local contribution to the energy predominates upon the formation of the chemical bond.[8—10]

The type of chemical bonding in a molecular system can be determined within the framework of the AM theory from the sign of $\nabla^2\rho(\mathbf{r})$ and the local electron energy $E(\mathbf{r})$ at the CPs (3, −1).[9,10] The bonds are classified in shared (covalent) bonds if $E(\mathbf{r}) < 0$ and $\nabla^2\rho(\mathbf{r}) < 0$ and bonds corresponding to closed-shell interactions if $E(\mathbf{r}) > 0$ and $\nabla^2\rho(\mathbf{r}) > 0$.[10] From Eq. (1) it follows that the Laplacian $\nabla^2\rho(\mathbf{r})$ can also take positive values at negative $E(\mathbf{r})$. Hence, a specific intermediate type of interactions characterized by $E(\mathbf{r}) < 0$ and $\nabla^2\rho(\mathbf{r}) > 0$ is distinguished.

Using 3-acetyl-4-hydroxycoumarin (**1**) as an example, in the present study we analyze (within the framework of the AM theory, which was briefly outlined above) the agreement between the results of quantum-chemical calculations of isolated systems containing strong intramo-

* The presence of the CPs (3, −1) in the interatomic space is a necessary and sufficient criterion for the formation of a chemical bond.[8] At this point, the Hessian has non-zero eigenvalues and the algebraic sum of their signs is equal to −1.

Published in Russian in *Izvestiya Akademii Nauk. Seriya Khimicheskaya,* No. 3, pp. 400—412, March, 2001.

1066-5285/01/5003-418 $25.00

lecular H-bonds and the data of X-ray diffraction studies of the corresponding crystals. We also elucidated the question of whether the calculated barrier to proton transfer always corresponds to the occurrence of the tautomeric equilibrium in the crystal.

Results and Discussion

Recent X-ray diffraction study of 3-acetyl-4-hydroxycoumarin at 153 and 298 K[11] has demonstrated that tautomer **1A** with an intramolecular H-bond (O...O 2.442 Å) (Scheme 1) predominates in the crystal. An analogous conclusion was drawn based on the results of photoelectron spectroscopy of compound **1** in the gas phase.[11] However, the complex shape of the ionization bands (broadening) did not rule out the presence of tautomer **1B** since the first ionization potentials calculated for tautomers **1A** and **1B** by the semiempirical AM1 method were found to be close (9.17 and 9.04 eV, respectively; *cf.* the experimental value of 9.10 eV). According to the HF/6-31G(d,p) quantum-chemical calculations,[11] tautomer **1A** has a lower energy than **1B**; however, the energy difference is less than 1 kcal mol^{-1}. Apparently, rapid proton transfer in the tautomers can occur both in the gas phase and in the crystal. However, calculations by the HF method did not reproduce the experimental geometry of molecule **1** and gave the substantially overestimated O...O distance (2.515 Å) and an underestimated degree of equalization of the bond lengths in the H-bonded six-membered ring.

Scheme 1

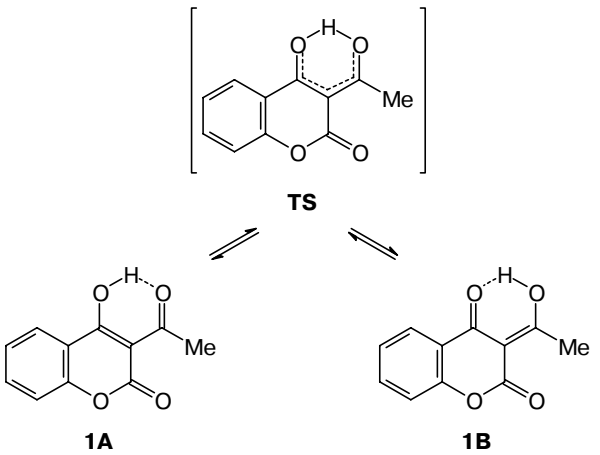

Static or dynamic disorder of the central H atom is highly probable to be observed in X-ray diffraction studies of such systems containing strong short H-bonds. This disorder occurs due to either the presence of both tautomers or rapid proton transfer in the crystals (see, for example, the data for acetylacetone[12]). In both cases, the superposition of the tautomers in the unit cell must lead to equalization of the effective bond lengths in the crystal, thus modeling the 4e,3c-hydrogen bonding. The symmetry of the position occupied by the molecule in the crystal can also lead to substantial disorder. Hence, when interpreting the results of X-ray diffraction studies of such systems, special attention should be given to analysis of anisotropic atomic displacement parameters in crystals.[12]

Hirshfeld's test[13] is one of the most frequently used criteria for the ordered/disordered arrangement of molecules in crystals. According to this criterion, the differences (Δ) between the mean-square amplitudes of the "oncoming" atomic displacements for pairs of atoms linked by chemical bonds (except for H atoms) in ordered crystal structures should be no larger than $\sim 10 \cdot 10^{-4}$ $Å^2$. In particular, the X-ray data for acetylacetone demonstrated that the symmetry plane (the space group *Pnma*, $Z = 4$) in the crystal passes through the midpoint of the O...O line (the O...O distance is 2.547(1) Å) perpendicular to the plane of the molecule. This fact does not allow the direct elucidation of the nature of disorder even based on the X-ray diffraction data collected at different temperatures. This conclusion was confirmed not only by the results of analysis of difference electron density maps in the region of the H-bond, but also by high Δ values (from $17 \cdot 10^{-4}$ to $56 \cdot 10^{-4}$ $Å^2$) for the bonds in the H-bonded six-membered ring observed throughout the experimental temperature range (110—210 K). Therefore, the above-mentioned symmetry plane in the acetylacetone molecule results from the superposition of two equivalent tautomers rather than from the formation of the 4e,3c-hydrogen bond.[12] The results of analysis of thermal motion of the atoms in the crystal of acetylacetone at 110 and 210 K agree well with those of IR studies carried out at different temperatures and with the results of quantum-chemical calculations performed with the complete basis set (CBS-4).[1]

Analogous analysis[11] of the amplitudes of the "oncoming" atomic displacements in molecule **1** at 153 K demonstrated that most of the bonds in the keto-enol fragment do not satisfy Hirshfeld's criterion (the average Δ value is $15 \cdot 10^{-4}$ $Å^2$), which may be indicative of the presence of an insignificant amount of tautomer **1B** in the crystal. Taking into account the results obtained for **1** by photoelectron spectroscopy in the gas-phase and the Δ values for the crystal of **1** at 153 K and in view of the fact that the barrier to proton transfer obtained from HF/6-31G(d,p) calculations[11] is low, in this work we carried out an X-ray diffraction study of the same single crystal of compound **1** in a wide temperature range (100—353 K) in order to elucidate the character of the tautomeric equilibrium in the crystal.

Since reliable estimates of the experimental geometry of systems with H-bonds can be obtained only in quantum-chemical calculations with inclusion of electron correlation (see, *e.g.*, Ref. 14), the tautomers **1A** and **1B** and the proton transfer in molecule **1** were studied within the framework of the density functional theory

Table 1. Selected crystallographic parameters and characteristics of the refinement of the crystal structure of **1** at 100—353 K

Parameter	100 K	200 K	300 K	353 K
Molecular weight		204.17		
$F(000)$		424		
Space group		$P2_1/c$		
a/Å	10.1990(2)	10.2473(7)	10.3193(9)	10.371(2)
b/Å	5.154(1)	5.1551(3)	5.1605(5)	5.1525(8)
c/Å	16.7930(3)	16.913(1)	17.071(1)	17.194(3)
β/deg	100.617(1)	100.075(1)	99.337(2)	98.855(4)
V/Å^3	867.67(3)	879.7(1)	897.0(1)	907.8(4)
d_{calc}/g cm^{-3}	1.563	1.542	1.512	1.494
μ(Mo-Kα)/cm^{-1}	1.21	1.19	1.17	1.15
$2\theta_{max}$/deg	98	60	60	60
Number of measured reflections	21588	8786	8768	9350
Number of independent reflections (R_{int})	7587 (0.023)	2520 (0.019)	2517 (0.020)	2621 (0.031)
wR_2 calculated based on F^2 using all reflections	0.1616	0.1359	0.1301	0.1493
R_1 calculated based on F (using reflections with $I > 2\sigma(I)$)	0.0614* (4914)	0.0454 (1902)	0.0451 (1566)	0.0481 (1456)
GOF	1.004	1.002	0.929	0.911

* The R_1 value calculated using the data of the multipole refinement using 3220 reflections with $I > 3\sigma(I)$ and $\sin\theta/\lambda < 0.90$ Å^{-1} was 0.038.

with the three-parameter B3LYP functional and the 6-31G(d,p) basis set using the GAUSSIAN-94W program package.[15]

Analysis of thermal vibrations in the crystal of 1

Judging from the changes in the parameters and unit cell volume (Table 1) of the crystal of **1** (Fig. 1) at 100—353 K, no phase transition occurs in this temperature range. Analysis of the anisotropic atomic displacements in molecule **1**, which was performed using the THMA-11 program[16] within the framework of the LTS model,[17] demonstrated that the molecule remains structurally rigid at all temperatures (the R_u values varied from 4.6 to 6.5%). The calculated differences between the mean-square amplitudes of the "oncoming" displacements (Δ) indicate that the bond lengths in both the keto-enol fragment and the remaining part of the molecule determined at 100 K satisfy Hirshfeld's criterion (the average values are $5.3 \cdot 10^{-4}$ and $6.3 \cdot 10^{-4}$ Å^2, respectively). A rise in the temperature leads to an increase in the Δ values for the keto-enol fragment to $15.3 \cdot 10^{-4}$, $16.5 \cdot 10^{-4}$, and $18.0 \cdot 10^{-4}$ Å^2 at 200, 300, and 353 K, respectively. The Δ values for all other C—C and O—C bonds are increased to $12.8 \cdot 10^{-4}$, $17.8 \cdot 10^{-4}$, and $19.8 \cdot 10^{-4}$ Å^2, respectively, for the same three temperatures.

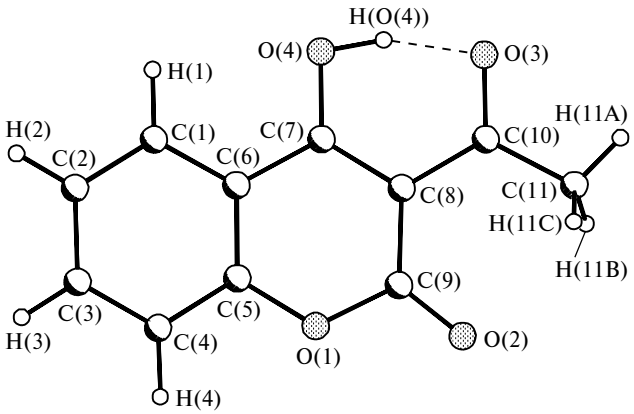

Fig. 1. Overall view of the 3-acetyl-4-hydroxycoumarin molecule.

Therefore, analysis of the anisotropic thermal parameters of the atoms in the single crystal of **1** suggests with a fair degree of assurance that the molecules are ordered at 100 K (from the viewpoint of the fixed position of the central H atom). Hence, proton transfer along the O(3)...O(4) line at 100 K is either absent or its contribution is negligible. This result allows the correct investigation of the character of chemical bonds in the compound under consideration by analyzing the electron density distribution in the crystal. This investigation was impossible, in particular, in the case of the crystals of acetylacetone[12] due to disorder of the molecules imposed by the crystal symmetry.

It was of interest to compare the Δ values for compound **1** with the analogous values for the keto-enol systems containing strong H-bonded six-membered rings for which the ρ(**r**) functions and the thermal motion in the crystals have also been analyzed. These data are available for benzoylacetone[17—19] (**2**) (the O...O distance is 2.502(4) Å) and citrine (**3**)[20] containing two keto-enol systems with the intramolecular O...O distances of 2.533 and 2.473 Å.

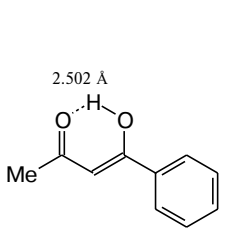

2

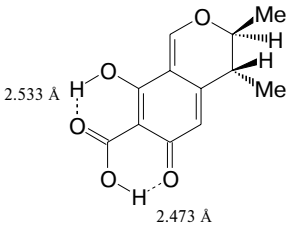

3

Analysis of the Δ values in the crystal of compound **2** [17] in the temperature range from 8 to 300 K demonstrated that Hirshfeld's criterion is fulfilled only at $T = 8$ K (the average Δ value is $7.0 \cdot 10^{-4}$ Å^2 and the maximum value for one of two C—O bonds is $10 \cdot 10^{-4}$ Å^2). On the contrary, a neutron diffraction study[17] at 20 K and X-ray diffraction study at 143 K showed that the Δ values for the bonds in the keto-enol

fragment are $13.6 \cdot 10^{-4}$ and $31.4 \cdot 10^{-4}$ Å^2, respectively (at 20 K, the maximum Δ value is $40 \cdot 10^{-4}$ Å^2) and the Δ values for the benzene ring are $7.8 \cdot 10^{-4}$ and $6.5 \cdot 10^{-4}$ Å^2, respectively. Despite the high Δ values for the crystal of **2** at 20 K, the authors[18,19] assumed that the molecules are ordered and used the position of the H atom, which was determined by neutron diffraction analysis at 20 K, for examination of the electron density distribution in the crystal at 8 K.[18,19] According to the results of X-ray diffraction study at 19 K, the Δ values for all bonds in molecule **3** are no larger than $6 \cdot 10^{-4}$ Å^2.[20]

It was of interest to analyze the temperature dependence of thermal ellipsoids in the H-bonded ring of molecule **1** (Fig. 2). At 100 K, the thermal ellipsoid of the central H(O(4)) atom is directed virtually perpendicular to the O(3)...O(4) line (the angle is ~80°). When the temperature was increased, the maximum amplitude of the displacement of the H(O(4)) atom was observed along the line of the H-bond, which may be evidence that partial migration of this atom occurs in the crystal at higher temperatures. At 100 K, the amplitudes of the "oncoming" displacements of the H(O(4)) atom for the O(4)—H(O(4)) and H(O(4))—O(3) bonds (0.016 and 0.049 Å^2, respectively) in the crystal of **1** are substantially smaller than the corresponding values in the crystal of **2** at 20 K (0.09 Å^2).[17] This signifies that the vibration amplitude of the H atom involved in hydrogen bonding in the crystal of **1** (0.18 Å) is nearly half as large as that in the crystal of **2** (0.30 Å). It should be noted that in the case of the superposition of two tautomers of benzoylacetone, the distance between two positions of the H atom is ~0.5 Å and, hence, residual disorder is observed in the crystal of **2** even at 20 K.

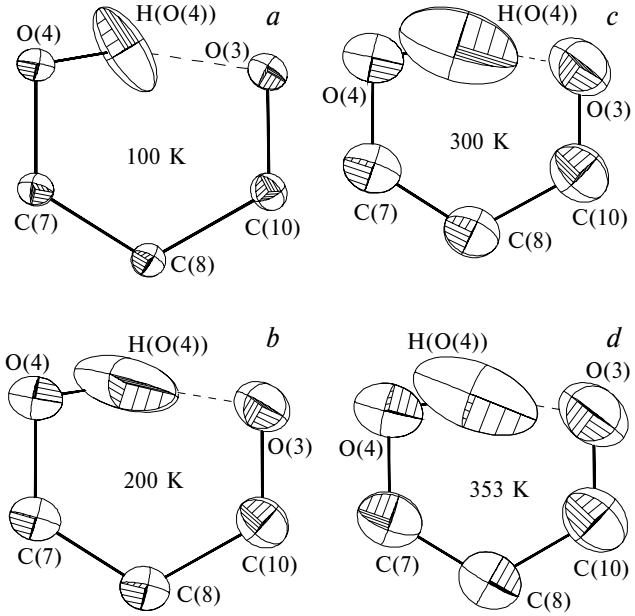

Fig. 2. Central ring in **1**; the atoms are represented as probability ellipsoids (p = 50%) of thermal vibrations at 100—353 K.

Geometry of molecule 1

The geometry of molecule **1** remains virtually unchanged as the temperature increases from 100 to 353 K. To take into account the effective shortening of the bonds due to thermal vibrations of the atoms, the libration corrections were calculated within the framework of the LTS rigid-body model. As can be seen from Table 2, the bond lengths and bond angles remain unchanged as the temperature rises even if the libration corrections are applied. Insignificant changes are observed only for the O—H bonds. However, the changes in the H(O(4))—O(4) and H(O(4))—O(3) distances observed in this case cannot be considered as a tendency for their equalization because the positions of the H atoms were determined in X-ray diffraction studies with an insufficient accuracy. An analogous situation has been observed previously[17] in the study of the crystal structure of **2**.

In the crystal, molecule **1** is planar with the C(11)C(10)O(3) acetyl group being slightly rotated (by 6.2°) relative to the 4-hydroxycoumarin fragment. The methyl group is antiperiplanar to the C(10)—O(3) bond. The bond lengths in the O(3)—C(10)—C(8)—C(7)—O(4) keto-enol fragment are indicative of a substantial electron density delocalization, which is manifested in the elongation of the formally double C(10)—O(3) and C(8)—C(9) bonds and in the shortening of the single C(10)—C(8) and C(7)—O(4) bonds compared to the "ideal" values for the C—O, C=O, C—C, and C=C bonds.[21] This type of the bond length distribution is typical of keto-enol systems. It was established[21—24] that the degree of electron density delocalization in the keto-enol fragment correlates with the energy (strength) of the intramolecular H-bond.

Analysis of the bond lengths in *cis*-enols of β-diketones based on the data for 20 structures* demonstrated[21—24] that the shortening of the O...O distance correlates with the degree of delocalization of the π-electron density in the H-bonded ring. The differences between the C—O and C=O distances (q^1) and between the C=C and C—C distances (q^2) were analyzed.[21] Since the q^1 and q^2 values are linearly interdependent, the parameter $Q = q^1 + q^2$, which characterizes the degree of delocalization of the π-electron density in the keto-enol system, was used. The condition $Q = 0$ corresponds to the completely delocalized system, whereas $Q = 0.320$ or -0.320 corresponds to the completely localized keto-enol or enol-ketone systems, respectively.

However, statistical analysis of a wider range of compounds, including the molecules in which the formally double C=C bonds are involved in the ring, revealed no correlation similar to that found previously.[21,22] Analysis of the structures of *cis*-enols of β-diketones in which the C—C bonds are either involved or not involved in the ring (a total of 240 structures),

* Analysis was carried out for ordered crystal structures with the localized central H atom with $R < 0.065$ and provided that the C=C and C—C bonds are not involved in the ring.[21—24]

Table 2. Principal bond lengths (d) and bond angles (ω) in **1** according to the X-ray diffraction data at 100—353 K and the total energies (E_{tot}) and zero-point energy (ZPE) corrections obtained from B3LYP/6-31G(d,p) quantum-chemical calculations

Parameter	**1A**	**1**				**1B**[a]	**TS**[a]
		100 K	200 K	300 K	353 K		
Bond				d/Å[b]			
O(3)...O(4)	2.447	2.4404(5) 2.442	2.442(1) 2.445	2.442(1) 2.447	2.444(1) 2.451	2.431	2.360
O(3)—C(10)	1.254	1.2593(7) 1.261	1.253(1) 1.257	1.255(1) 1.262	1.253(2) 1.259	1.303	1.282
O(4)—C(7)	1.311	1.3091(6) 1.311	1.305(1) 1.309	1.304(2) 1.309	1.300(2) 1.307	1.262	1.282
O(4)—H(O(4))	1.032	0.95(1) 0.972	0.99(2)	1.02(3)	1.05(3)	1.446	1.227
H(O(4))—O(3)	1.485	1.52(1) 1.433	1.49(2)	1.45(3)	1.42(3)	1.046	1.179
C(7)—C(8)	1.403	1.4005(8) 1.402	1.399(1) 1.402	1.396(2) 1.403	1.398(2) 1.403	1.447	1.427
C(6)—C(7)	1.446	1.4433(7) 1.444	1.443(1) 1.445	1.442(2) 1.444	1.440(1) 1.443	1.461	1.453
C(8)—C(9)	1.458	1.4518(7) 1.454	1.451(1) 1.455	1.452(2) 1.452	1.446(2) 1.453	1.460	1.455
C(8)—C(10)	1.463	1.4555(7) 1.456	1.454(1) 1.456	1.449(2) 1.459	1.446(2) 1.450	1.409	1.429
O(1)—C(5)	1.360	1.3687(7) 1.370	1.370(1) 1.373	1.365(1) 1.370	1.366(2) 1.371	1.367	1.364
O(1)—C(9)	1.400	1.3833(7) 1.384	1.385(1) 1.387	1.381(2) 1.384	1.383(2) 1.386	1.392	1.397
O(2)—C(9)	1.210	1.2145(7) 1.215	1.207(1) 1.210	1.203(2) 1.208	1.202(2) 1.221	1.212	1.211
C(10)—C(11)	1.503	1.4947(8) 1.496	1.489(2) 1.492	1.485(2) 1.491	1.482(2) 1.488	1.494	1.496
Bond angle				ω/deg			
O(3)—H(O(4))—O(4)	152.4	161(1)	161(1)	161(2)	161(2)	152.4	157.5
H(O(4))—O(4)—C(7)	104.6	100(1)	99(1)	99(1)	99(1)	100.5	101.5
H(O(4))—O(3)—C(10)	103.6	99.5(6)	99.7(7)	99.7(9)	99.7(9)	106.0	104.3
O(3)—C(10)—C(8)	119.3	119.03(5)	119.0(1)	118.9(1)	119.0(1)	119.8	118.7
O(3)—C(10)—C(11)	118.5	118.41(5)	118.6(1)	118.2(1)	118.0(1)	114.9	117.0
C(7)—C(8)—C(10)	118.1	118.31(5)	118.4(1)	118.7(1)	118.8(1)	117.9	116.9
O(4)—C(7)—C(8)	122.0	122.00(5)	122.1(1)	122.1(1)	121.9(1)	121.8	121.1
C(8)—C(9)—O(1)	116.8	117.76(5)	117.6(1)	117.5(1)	117.7(1)	116.9	116.6
C(9)—O(1)—C(5)	123.1	122.42(4)	122.5(1)	122.7(1)	122.7(1)	123.0	123.0
C(8)—C(9)—O(2)	127.2	127.05(5)	127.3(1)	127.3(1)	127.3(1)	126.7	127.0
O(1)—C(9)—O(2)	116.1	115.18(5)	115.1(1)	115.2(1)	114.9(1)	116.4	116.4
				E_{tot}/a.u.			
Energy of the molecule	−724.930525					−724.929394	−724.928575
				ZPE/kcal mol^{-1}			
Zero-point energy	106.38(0)[c]					106.24(0)[c]	104.27(1)[c]

[a] The atomic numbering scheme for the tautomers of **1** and for the transition state (**TS**) are identical with that used for the tautomer of **1** shown in Fig. 1.
[b] The bond length determined by X-ray diffraction analysis are given without libration corrections (the first line) and with inclusion of these corrections (the second line).
[c] The number of imaginary frequencies is given in parentheses.

which were chosen from the Cambridge Structural Database (CSD, 2000) based on the same criteria, demonstrated that the correlation coefficient between the Q parameter and the O...O distance is only ~0.57. The correlation coefficients for the structures in which the C=C bond is either involved in the ring (a total of 58 structures) or belongs to the aromatic system (a total of 134 structures) are 0.59 or 0.14, respectively.

These correlations do not hold for structures **1—3**. A comparison of the Q values for **1** and **3** showed that, despite the shorter O...O distance in **1** compared to that in **3**, the Q value is smaller for **3** (0.105 and 0.073 Å for

1 and **3**, respectively). Analogously, the *Q* values for the H-bonded six-membered rings in molecules **2** (O...O 2.502 Å) and **3** (O...O 2.533 Å) are 0.016 and 0.091 Å, respectively.

The equalization of the bond lengths in molecule **2** compared to those in molecules **1** and **3** found from the B3LYP/6-311G(d,p) quantum-chemical calculations was attributed[19] to the low barrier to proton transfer. As a result, the energy of the H atom involved in hydrogen bonding is higher than the barrier top even at 8 K. The calculated barriers to proton transfer in molecule **2** are 1.7 and 2.4 kcal mol^{-1} for the enol-ketone and ketone-enol forms, respectively.[19] The inclusion of zero-point energy (ZPE) correction in calculations for the tautomers of **2** led to the situation where the transition state with the H atom occupying virtually the central position appeared to have the lower energy (−0.6 and −0.2 kcal mol^{-1}, respectively). This is in agreement with the assumption[19] that the migration of the H atom in **2** at 8 K is barrierless.

However, the inclusion of ZPE correction by addition of this parameter to the total energy is not quite correct because the imaginary frequency, which in this case corresponds to the vibration of the H atom along the hydrogen-bond line, is ignored in calculations of the ZPE correction for the transition state. Hence, the zero-point energy of the transition state is, undoubtedly, lower. According to one of the most widely used procedures,[14] the vibration frequency corresponding to the imaginary frequency in the transition state is ignored in calculations of the ZPE correction for the ground state. We used this procedure for the estimation of the barrier to proton transfer based on the published data[19] and obtained the larger values for molecule **2** (~3.6 and 4.1 kcal mol^{-1} for enol-ketone and ketone-enol, respectively). However, in spite of the above-mentioned differences in the barriers to proton transfer and their probable dependence on both the basis set and the calculation procedure (see, *e.g.*, Ref. 1), it is believed that the symmetrical H-bond can be present in the crystal of **2** even at 8 K.

It should be noted that the data of X-ray and neutron diffraction investigations of compound **2** [17—19] are not in complete agreement with the results of NMR studies,[25—27] which, in particular, indicate that the H-bond both in solution and in the crystal is most likely described by a double-well potential. For instance, analysis of the changes in the chemical shifts $\Delta\delta(^1H,^2H)$ and $\Delta\delta(^1H,^3H)$ upon isotopic replacement of the hydrogen atom by the deuterium or tritium atom disclosed that the $\Delta\delta(^1H,^2H)$ and $\Delta\delta(^1H,^3H)$ values for benzoylacetone are much the same as those observed for acetylacetone (0.61 and 0.67, respectively)[25] and that the isotope effect for these molecules (1.34 and 1.39, respectively) corresponds to the effect observed for H-bonds with the double-well potential (1.44). Since the H-bond in acetylacetone is described by the double-well potential (see Refs. 1 and 12), the results obtained in the study[25] suggest that the H-bond in benzoylacetone should be similar in character. Analysis of the ^{13}C and ^{17}O NMR spectra of benzoylacetone in the solid state and its solutions, which provided evidence for the differences in the O and C atoms in the keto-enol ring, led to the same conclusion.[26,27]

Assuming that equalization of the bond lengths in **2** [17] is not due to the superposition of the tautomers in the crystal and taking into account a lesser degree of the electron density delocalization in the crystal of **1**, one would expect that the barrier to proton transfer in **1** will be substantially higher than that in **2**. To evaluate the barrier height in **1**, we performed quantum-chemical calculations of tautomers **1A** and **1B**.

Proton transfer in molecule 1

Unlike the results of HF calculations,[11] the results of B3LYP/6-31G(d,p) calculations with inclusion of electron correlation are in good agreement with the experimental geometry (see Table 2). For instance, the calculated O(3)...O(4) distance in tautomer **1A** is 2.447 Å (*cf.* the experimental values of 2.442—2.451 Å). In tautomer **1B**, the proton transfer leads to an insignificant shortening (by 0.016 Å) of the O(3)...O(4) distance. It can be assumed that the hydrogen bond in tautomer **1B** is stronger than that in tautomer **1A**, which is consistent with a higher degree of delocalization of the π-electron density (*Q* is 0.117 and 0.079 Å in **1A** and **1B**, respectively) and with the ratio between the ν(OH) vibration frequencies calculated in the same approximation (2628.5 cm^{-1} for **1A** and 2409.6 cm^{-1} for **1B**). The energy of the hydrogen bond (E_{HB}) in **1B** calculated with the use of the dependence proposed[28] for *cis*-enols of β-diketones (E_{HB}/kcal mol^{-1} = 58.77(3640 − ν(OH))/3640) is 3.5 kcal mol^{-1} higher than that in **1A**.

According to the published data,[21—24] tautomer **1B** with the stronger H-bond should be more stable than tautomer **1A**. However, we found that the energy of tautomer **1B** calculated with inclusion of ZPE correction is ~0.6 kcal mol^{-1} higher than that of tautomer **1A**. An analogous situation was also observed for compound **2** in which the energetically more favorable tautomer (the energy difference is ~0.7 kcal mol^{-1})[19] also has a higher (by 90 cm^{-1}) ν(OH) vibration frequency and is characterized by a larger (by 0.01 Å) O...O distance. A comparison of the ν(OH) frequencies in **1A**, **1B**, and **2** revealed a weaker H-bond in compound **2**.

Calculations for the isotopically substituted (H/D) tautomers **1A** and **1B** gave the expected decrease in the ν(OH) vibration frequencies down to 1944.5 and 1822 cm^{-1}, respectively. The isotope effect is 1.35 for **1A**, 1.32 for **1B**, and 1.36 for **2**. These values are typical of double-well potentials for H-bonds.[5]

Examination of the potential surface of proton transfer demonstrated that the transition state (**TS**) corresponds to the symmetrical arrangement of the proton

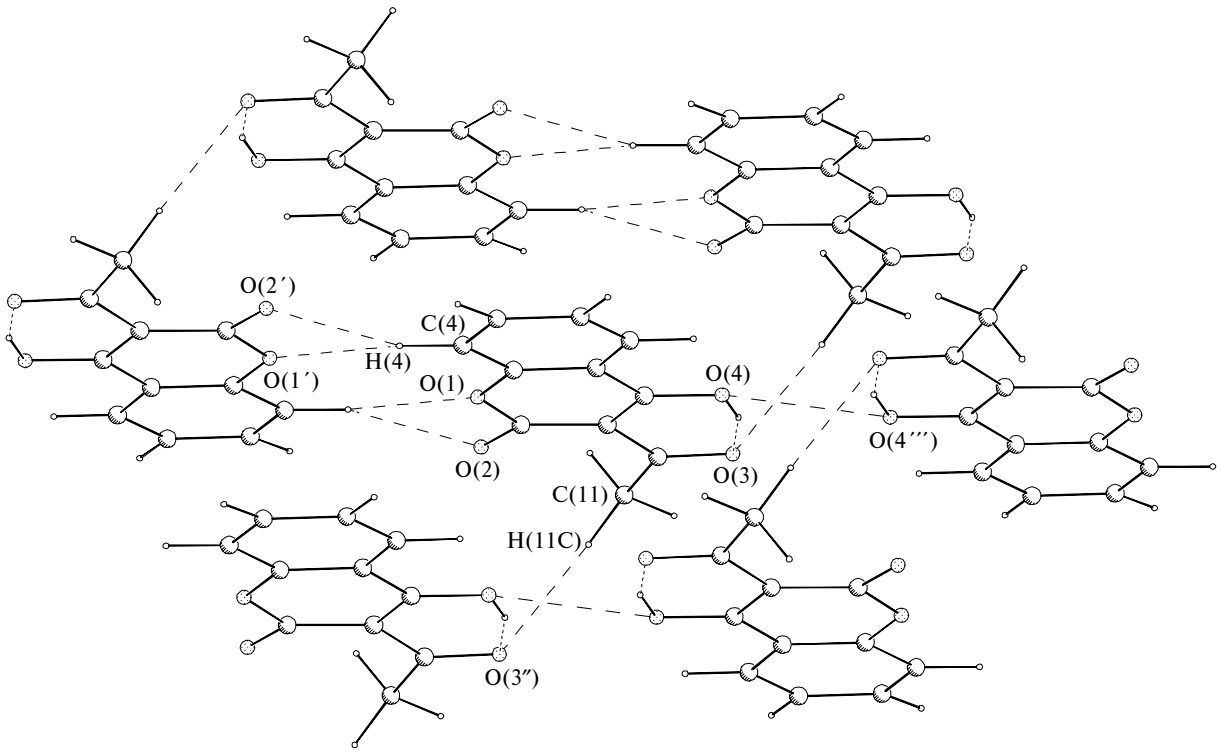

Fig. 3. The C—H...O contacts and interactions between the hydroxy groups in the crystal of 3-acetyl-4-hydroxycoumarin.

between the O(3) and O(4) atoms. Analysis of the frequencies performed within the framework of the B3LYP/6-31G(d,p) method demonstrated that the vibration frequency of the H(O(4)) atom along the H-bond line in the transition state is imaginary (i837.0 cm^{-1}). The nearly symmetrical arrangement of the H atom (the H(O(4))—O(4) and H(O(4))—O(3) distances are 1.227 and 1.179 Å, respectively) is accompanied by virtually complete equalization of the bond lengths in the keto-enol ring (Q = 0.002) and by a substantial shortening of the O(3)...O(4) distance (down to 2.360 Å). It is noteworthy that the shortest O—H distance in the **TS** is observed for the "hydroxy group" of energetically less favorable tautomer **1B**.

Such a shortening of the O...O distance in the **TS** seems to be a common feature of keto-enol systems. According to the published data,[1,19] the O...O distances in the **TS** of proton transfer are 2.359 and 2.363 Å for molecule **2** and acetylacetone, respectively. However, such very short O...O distances are not observed in the crystal structures of *cis*-enols. In particular, despite the close values of the calculated C—O and C—C bond lengths in the crystal of **2** and in the **TS**, the O...O distance in the crystal is 0.14 Å longer than that in the **TS**. Surprisingly, this difference has previously been estimated as insignificant.[19]

A comparison of the energies of tautomers **1A** and **1B** and of the **TS** demonstrated that the barriers to proton transfer **1A**→**TS** and **1B**→**TS** calculated without ZPE correction are ~1.2 and 0.5 kcal mol^{-1}, respectively, whereas these barriers calculated with inclusion of ZPE correction are 2.9 and 2.0 kcal mol^{-1}, respectively. Therefore, the barrier to proton transfer in molecule **1** is even lower than that in **2**, which, by analogy with the latter, should result in equalization of the bond lengths in the H-bonded six-membered ring at 100 K. However, this equalization was not experimentally observed (see Table 2).

Crystal structure of 3-acetyl-4-hydroxycoumarin

It cannot be ruled out that intermolecular interactions in the crystal of **1** can lead to the preferential stabilization of one of the tautomers and its predominance at 100 K. Actually, analysis of the crystal packing* of **1** (Fig. 3) demonstrated that the molecules are linked in dimers through bifurcated C—H...O contacts, *viz.*, C(4)—H(4)...O(1′) (−x, 1 − y, 1 − z) and C(4)—H(4)—O(2′) (−x, 1 − y, 1 − z) (C(4)...O(1′), 3.523(1) Å; H(4)...O(1′), 2.51 Å; C(4)H(4)O(1′), 157°; C(4)...O(2′), 3.404(1) Å; H(4)...O(2′), 2.44 Å; C(4)H(4)O(1′), 149°). The dimers, in turn, are linked in layers through analogous contacts between the H atoms of the methyl group and the O(3) atom of the keto-enol

* All geometric parameters are given for **1** at 100 K. The geometric characteristics of the C—H...O contacts were calculated with the use of the C—H bonds normalized to 1.07 Å according to the neutron diffraction data.

fragment (C(11)—H(C(11))...O(3″) (x, $-1 + y$, z); C(11)...O(3″), 3.535(1) Å; H(C(11))...O(3″), 2.47 Å; C(11)H(C(11))O(3), 177°)).

In addition to the above-mentioned contacts, a number of other interactions involving the keto-enol system, in particular, the shortened intermolecular contact (2.849(1) Å) formed by the O(4)H(O(4)) hydroxy groups (O(4)...O(4‴) ($1 - x$, $3 - y$, $1 - z$), are observed in the crystal structure of **1**. In spite of the fact that the maximum vibration amplitude of the H(O(4)) atom (see Fig. 2) at 100 K is observed along the O(4)...O(4‴) line, it is highly improbable that the latter contact results from the intermolecular interaction between the H(O(4)) and O(4‴) atoms because the H(O(4))...O(4‴) distance in **1** is rather large (2.59 Å) and the O(4)—H(O(4))—O(4‴) bond angle is 92°. On the other hand, intermolecular interactions between the keto-enol H-bonded rings (Fig. 4) (the shortest O(3)—C(7⁗) ($1 - x$, $2 - y$, $1 - z$) and O(4)—C(10⁗) ($1 - x$, $2 - y$, $1 - z$) distances are 3.218 and 3.190 Å, respectively) occur within the layers described above. In these layers, the H-bonded rings are parallel to one another and their centers are separated by 3.280 Å. Taking into account substantial delocalization of the π-electron density in the keto-enol ring (see above), it is reasonable to consider this interaction as a stacking interaction.

Analysis of the data available in CSD (the structures were chosen based on the above-mentioned boundary conditions) demonstrated that similar *trans* arrangements (see Fig. 4) of the keto-enol rings occur rather frequently. This type of arrangement was found in 55 ordered crystal structures of intramolecularly H-bonded *cis*-enols of β-diketones in which the distances between the centers of the H-bonded rings are in the range of 3.16—3.61 Å. However, no correlation between the O...O distances and the separations between the centers of the H-bonded rings was found.

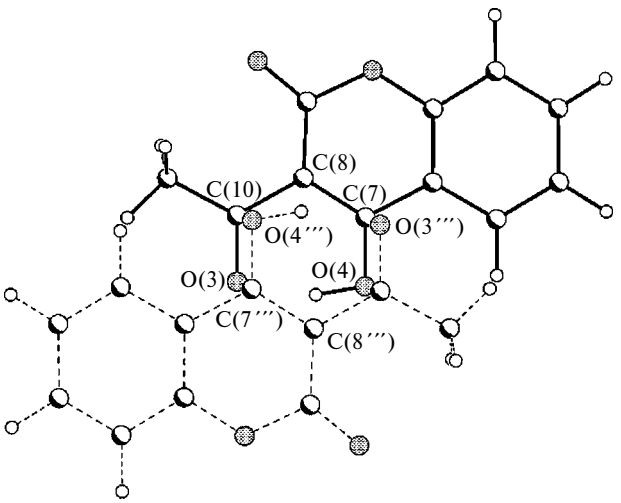

Fig. 4. Illustration of the interaction between the π-systems of the H-bonded keto-enol rings in the crystal of 3-acetyl-4-hydroxycoumarin.

This type of intermolecular interactions in *cis*-enols of β-diketones has not been investigated previously. However, analogous interactions between the carbonyl groups have been reported.[29] Analysis of the data available in the CSD diclosed that these interactions are characterized by a specific directionality (the parallel arrangement of the C=O bonds) and in some cases can compete with the formation of H-bonds. The energy of the interaction between the carbonyl groups, which was calculated in the case of their parallel arrangement and with the C...O distances varying from 3.0 to 3.30 Å, ranges from 5 to 3 kcal mol^{-1}.[29]

Intermolecular interactions analogous to those found in the crystal structure of **1** were also observed in the crystal of **2**.[17] Analysis of the crystal packings of **1** and **2** revealed the similarity of intermolecular interactions in these crystals (primarily, the shortened contacts involving the six-membered H-bonded rings). These contacts seem to have a similar effect on the proton transfer along the H-bond line. Hence, neither the heights of the barriers to proton transfer nor the characteristic features of the crystal packing can be responsible for a substantial difference in the degree of delocalization of the π-electron density in **1** and **2**.

Topological analysis of the electron density distribution in the crystal of 1

The character of interatomic interactions in the region of the hydrogen bond in the crystal of **1** was examined using the topological analysis of the electron density distribution function. Analysis was performed based on the multipole refinement of the X-ray diffraction data collected at 100 K and on the results of quantum-chemical calculations for tautomers **1A** and **1B** and for the **TS** of proton transfer by the density functional method (B3LYP/6-31G(d,p)). It is known that the H...B interactions in most systems with hydrogen bonds (A—H...B) are characterized by the positive Laplacian of the electron density $\nabla^2\rho(\mathbf{r})$ at the CP (3, −1) and that these interactions belong to closed-shell interactions.[30—33] According to the results of quantum-chemical calculations, the exceptions are only H-bonds in the FHF^-, $H_5O_2^+$, and $H_3O_2^-$ ions in which interactions between the central H atom and the adjacent atoms are characterized by the negative $\nabla^2\rho(\mathbf{r})$ values[34] and, hence, these ions possess symmetrical 4e,3c-hydrogen bonds.

However, the question of whether the H atom is located symmetrically remains open even in the case of strong H-bonds. For example, the symmetrical location of the hydrogen atom and the C_s symmetry of the cation were obtained in the calculations for $H_5O_2^+$ at the MP2 and MP4 levels of theory.[34] On the other hand, calculations performed using one of the most correct procedures for the description of electron correlation within the framework of the coupled cluster theory (B-CCD(T)) showed that configurations with the symmetry C_s and C_2 correspond to the **TS** and the equilibrium geometry,

respectively.[35] These calculations also led to an unsymmetrical arrangement of the proton; the O—H distances are 1.262 and 1.129 Å and the O...O distance is 2.3896 Å.

A different situation is observed in X-ray diffraction studies of crystals with strong H-bonds. In a series of recent experimental investigations of strong O—H—O bonds, it has been demonstrated that both O—H interactions are characterized by negative $\nabla^2\rho(\mathbf{r})$ values at the CPs (3, −1) and, hence, these interactions may be thought to be covalent.[18,19,36,37] This type of hydrogen bonding was found for the intramolecular O—H—O bonds in **2** [18,19] at 8 K (O...O, 2.502(4) Å) and in methylammonium monohydromaleate at 122 K (O...O, 2.4214(5) and 2.4183(5) Å)[36] and for the intermolecular H-bond in methylammonium monohydrosuccinate (O...O, 2.442(1) Å).[37]

In the crystal structures of the above-mentioned methylammonium salts, the H atom involved in hydrogen bonding occupies a special position on a symmetry plane. We calculated the amplitudes of the "oncoming" vibrations using anisotropic thermal parameters for the monohydrosuccinate anion (the space group $P2_1/m$) reported previously[37] and showed that the Δ values for the C—O bond involved in hydrogen bonding do not satisfy Hirshfeld's criterion ($\Delta = 41 \cdot 10^{-4}$ Å^2 for the results of neutron diffraction study and $\Delta = 21 \cdot 10^{-4}$ Å^2 for the data of X-ray diffraction study). Therefore, the presence of the crystallographic symmetry plane in this molecule, as in the crystal of acetylacetone,[12] precludes the elucidation of the nature of disorder. Consequently, the unusual topology of $\rho(\mathbf{r})$ (the negative Laplacian) in the region of the H-bond corresponds to the superposition of two molecules with an asymmetrical H-bond rather than to 4e,3c-hydrogen bonding.

Unfortunately, it is impossible to estimate the degree of ordering of monohydromaleate anions in the crystal[36] by analyzing the Δ values because the bond lengths and bond angles in the tautomers have close values[38] and the Δ values will satisfy Hirshfeld's criterion even in the case of the equiprobable superposition of the tautomers in the crystal. As was demonstrated by the MP2 quantum-chemical calculations of the monohydromaleate anion,[39] the "short" O—H bond in the equilibrium state with an asymmetrical H-bond is covalent ($\nabla^2\rho(\mathbf{r}) < 0$), whereas the "long" O—H bond corresponds to the closed-shell interaction ($\nabla^2\rho(\mathbf{r}) > 0$). The topological analysis of $\rho(\mathbf{r})$ in the salt of 1,2-dichloromonohydromaleate,[40] which is characteized by the shortest O...O distance (2.384 Å) of all known maleates and in which the central H atom occupies a general position, showed that both O—H bonds correspond to ionic interactions.[40]*

Therefore, the results obtained in the present investigation indicate that the data of X-ray and neutron diffraction studies do not generally allow one to unambiguously determine whether the symmetrical arrangement of the proton results from the formation of the 4e,3c-hydrogen bond or from the presence of static or dynamic disorder in the crystal, as in the case of acetylacetone[12] and the monohydrosuccinate anion.[36]

In addition, the question about the type of interactions in the region of the strong H-bond in the case of an asymmetrical arrangement of the proton remains open. As mentioned above, the positive value of the electron density Laplacian at the CP (3, −1) does not ensure that the interaction belongs to closed-shell interactions because within the framework of the AM theory its type is determined by the sign of the local electron density.[9] It should be emphasized that the $E(\mathbf{r})$ energies have not been analyzed in most of quantum-chemical calculations and this characteristic cannot be directly established in experimental studies. The rather small $\rho(\mathbf{r})$ and $\nabla^2\rho(\mathbf{r})$ values at the CPs (3, −1) usually serve as arguments in favor of the assignment of the H...B contact in the A—H...B hydrogen bond to closed-shell interactions. However, the correctness of this classification is doubtful because the estimates "rather small" and "rather large" are subjective.

Let us consider the results of the topological analysis of $\rho(\mathbf{r})$ in tautomers **1A** and **1B** and in the **TS** of proton transfer. We analyzed the results of our B3LYP/6-31G(d,p) calculations (Table 3). A search for the CPs using the EXTREME program[41] demonstrated that the CPs (3, −1) are located on all bonds including the intramolecular H-bond. According to Poincare—Hopf's relationship,[42] the formation of the H-bonded six-membered ring leads to the appearance of an additional CP (3, +1) localized within the ring. By analyzing the $\rho(\mathbf{r})$ and $\nabla^2\rho(\mathbf{r})$ values and the contributions of the kinetic and potential energies ($G(\mathbf{r})$ and $V(\mathbf{r})$) to the density of the electron energy (see Table 3), we found that, despite the negative $\nabla^2\rho(\mathbf{r})$ values at the CPs (3, −1) on some bonds, the density of the potential energy is higher than that of the kinetic energy for all interactions including the H-bonds in tautomers **1A** and **1B**. Thus, the Laplacian $\nabla^2\rho(\mathbf{r})$ at the CPs (3, −1) for the "long" H(O(4))...O(3) bond in tautomer **1A** and for the "long" H(O(4))...O(4) bond in tautomer **1B** has positive values (3.878 and 3.511 eÅ^{-5}, respectively) and the $\rho(\mathbf{r})$ values are small (0.559 and 0.619 eÅ^{-3}, respectively). The $E(\mathbf{r})$ energies for these bonds are negative (−0.022 and −0.031 a.u., respectively) For comparison, the $\rho(\mathbf{r})$, $\nabla^2\rho(\mathbf{r})$, and $E(\mathbf{r})$ values at the CPs (3, −1) for the "short" O—H bonds are 1.961 eÅ^{-3}, −35.619 eÅ^{-5}, and −0.450 a.u., respectively, for tautomer **1A** and 1.886 eÅ^{-3}, −32.551 eÅ^{-5}, and −0.420 a.u., respectively, for **1B**.

Thus, quantum-chemical calculations demonstrated that the H-bonds in both tautomers correspond to the intermediate type of interactions ($E(\mathbf{r}) < 0$ and $\nabla^2\rho(\mathbf{r}) > 0$). The results of topological analysis of $\rho(\mathbf{r})$ also indicate that the hydrogen bond in tautomer **1B** is, apparently, stronger, which is consistent with the geometry of the keto-enol ring and the behavior of the ν(OH)

* In the study,[40] the $\nabla^2\rho(\mathbf{r})$ values at the CPs (3, −1) in the region of the H-bond were not reported.

Table 3. Principal topological characteristics of tautomers **1A** and **1B** and of the **TS** at the CPs (3, −1) of the H-bonded six-membered ring according to the results of B3LYP/6-31G** calculations (I) and X-ray diffraction study (II) at 100 K

Bond	Tautomer	Method	$\rho(\mathbf{r})$/eÅ^{-3}	$\nabla^2\rho(\mathbf{r})$/eÅ^{-5}	$G(\mathbf{r})$/a.u.	$V(\mathbf{r})$/a.u.	$E(\mathbf{r})$/a.u.	ε
O(4)—H(O(4))	**1A**	I	1.961	−35.619	0.081	−0.531	−0.450	0.001
	1A	II	1.94	−13.76	0.265	−0.673	−0.408	0.02
	1B	I	0.619	3.511	0.068	−0.099	−0.031	0.001
	TS	I	1.126	−7.953	0.094	−0.270	−0.176	0.001
O(3)—H(O(4))	**1A**	I	0.559	3.878	0.062	−0.084	−0.022	0.001
	1A	II	0.554	5.229	0.081	−0.107	−0.026	0.02
	1B	I	1.886	−32.511	0.082	−0.502	−0.420	0.001
	TS	I	1.294	−13.231	0.094	−0.326	−0.232	0.001
O(4)—C(7)	**1A**	I	2.217	−7.350	0.456	−0.988	−0.525	0.02
	1A	II	2.58	−32.05	0.358	−1.048	−0.690	0.31
	1B	I	2.487	−3.335	0.582	−1.199	−0.617	0.02
	TS	I	2.380	−5.567	0.528	−1.112	−0.584	0.02
O(3)—C(10)	**1A**	I	2.522	−5.018	0.620	−1.246	−0.625	0.02
	1A	II	2.78	−32.65	0.430	−1.200	−0.770	0.20
	1B	I	2.278	−5.029	0.489	−1.031	−0.514	0.04
	TS	I	2.366	−3.640	0.541	−1.120	−0.579	0.02
C(7)—C(8)	**1A**	I	2.096	−20.360	0.102	−0.416	−0.314	0.26
	1A	II	1.95	−16.71	0.248	−0.670	−0.421	0.42
	1B	I	1.948	−17.906	0.081	−0.349	−0.267	0.18
	TS	I	2.022	−19.063	0.090	−0.378	−0.288	0.22
C(8)—C(10)	**1A**	I	1.890	−16.970	0.075	−0.326	−0.251	0.16
	1A	II	1.88	−13.73	0.247	−0.636	−0.389	0.29
	1B	I	2.069	−19.955	0.099	−0.405	−0.306	0.26
	TS	I	2.001	−18.822	0.089	−0.373	0.284	0.22
H-bonded ring	**1A**	I	0.136*	3.710*				
	1A	II	0.167*	3.20*				
	1B	I	0.187*	3.880*				
	TS	I	0.168*	4.361*				

* The characteristics of tautomers **1A** and **1B** and of the **TS** at the CPs (3, +1) in the region of the H-bonded ring.

frequencies. This is manifested both in the larger $\rho(\mathbf{r})$ value and in the magnitude of $E(\mathbf{r})$ at the CP (3, −1) (see Table 3). Analysis of the $G(\mathbf{r})$ and $V(\mathbf{r})$ contributions for the O—H and O...H bonds disclosed that the magnitude of $E(\mathbf{r})$ decreases due to a substantial decrease in the contribution of the potential energy to the local energy density, whereas the density of the kinetic energy for these bonds remains virtually the same. The topological parameters of the C—O and C=C bonds at the CPs (3, −1) in the keto-enol ring in tautomers **1A** and **1B** also reflect a more pronounced delocalization of the π-electron density in tautomer **1B**.

For the **TS** of proton transfer, the topological characteristics of $\rho(\mathbf{r})$ at the CPs (3, −1) are virtually identical for the pair of the O(4)—C(7) and O(3)—C(10) bonds as well as for the pair of the C(7)—C(8) and C(8)—C(10) bonds. As a result of substantial shortening of the O(3)...O(4) distance (2.360 Å) in the **TS** compared to those in tautomers **1A** (2.447 Å) and **1B** (2.431 Å), the sign of $\nabla^2\rho(\mathbf{r})$ at the CPs (3, −1) for both O—H bonds is negative and, hence, the 4e,3c-hydrogen bond occurs in the **TS**, unlike the tautomers **1A** and **1B**. Since the energy of the hydrogen bond is proportional to $\rho(\mathbf{r})$ at the CP (3, −1),[30] the results of calculations indicate that the O...H bonds in the **TS** are stronger than those in **1A** and **1B**, whereas the analogs of these bonds are weaker than the O—H bonds in **1A** and **1B**, the differences being of the same order of magnitude. Thus, the topological analysis of the electron density distribution in molecule **1** based on the data of quantum-chemical calculations demonstrated that, taking into account the short O...O distances in tautomers **1A** and **1B** (2.447 Å and 2.431 Å, respectively), the O...H bonds in these tautomers correspond to the intermediate type of interactions rather than to closed-shell interactions. This is likely responsible for both the low barrier to proton transfer and the high energy of the H-bond.

To estimate the difference in the electron density distribution in the crystal and in the gas phase and to find out whether the intermediate type of the interatomic O...H interaction is retained in the crystal, we performed the multipole refinement of the X-ray diffraction data for the crystal of **1** collected at 100 K. The analytical form of the function $\rho(\mathbf{r})$ was obtained using the Hansen—Coppens multipole model[43] in which the aspherical electron density of each atom is represented as the sum of the undistorted (spherically symmetrical) Hartree—Fock core and valence electron densities with the spherical harmonics that describe the deformation of

the valence shells upon the formation of a chemical bond:

$$\rho^{at}(\mathbf{r}) = P_{core}\,\rho^{at}_{core} + k'^3 P^{at}_{val}\rho^{at}_{val}(k'\mathbf{r}) + \\ + \sum_{l=0}^{l_{max}} k''^3 R_{kl}(k''\mathbf{r}) \sum_{m=-l_{max}}^{+l_{max}} P^{at}_{lm} Y^l_m(\theta,\phi),$$

Here, P_{core}, P_{val}, and P_{lm} are the multipole populations obtained by the least-squares method and k' and k'' are the expansion-contraction parameters of the valence shell and multipoles, respectively.[43] The total number of electrons belonging to one atom is $P_{core} + P_{valence} + P_{lm}$ (after space integration, the terms with $l \neq 0$ become equal to zero). The ρ_{core} and ρ_{val} functions are constructed from the Hartree—Fock AOs. The Slater functions were chosen as radial functions. The spherical harmonics ($Y_m{}^l(\theta,\phi)$) were normalized so that the population equal to unity corresponded to the transfer of one electron from the negative to positive lobes of the multipole.[43]

Analysis of the static deformation electron density (DED) maps demonstrated that the DED is accumulated in the regions of all covalent bonds and the lone electron pairs (LEP) of the O atoms in **1** (Fig. 5). For the O(3)...H(O(4)) hydrogen bond, both DED depletion in the vicinity of the H(O(4)) atom and the polarized maximum of the DED corresponding to the LEP of the O(3) atom are observed. This is typical of the DED for strong H-bonds with the asymmetrical location of the proton. The DED maximum corresponding to the LEP of the O(3) atom involved in hydrogen bonding is substantially lower than the peak corresponding either to the second LEP of this atom or to the LEP of the O(4) atom. This suggests that the covalent contribution to the O(3)...H(4) bond is rather large.

The distribution of $-\nabla^2\rho(\mathbf{r})$* (Fig. 6) shows that the electron density is accumulated in the regions of the chemical bonds and the LEP of the O atoms, whereas depletion of the electron density is observed in the vicinity of the H-bond, like in the DED map (see Fig. 5). Based only on the qualitative analysis of the distribution of $-\nabla^2\rho(\mathbf{r})$ in the region of the H-bond, it can be concluded that the H(O(4))...O(3) contact corresponds to a closed-shell interaction.

To correctly analyze the character of the interactions, we performed a search for the CPs in the crystal and found that the CPs (3, −1) are localized on all chemical bonds including the H(O(4))...O(3) bond, whereas the CPs (3, +1) are localized within the benzene and oxygen-containing rings and within the H-bonded six-membered ring. This is in agreement with the results of quantum-chemical calculations. As can be seen from Table 3, the $\rho(\mathbf{r})$ and $\nabla^2\rho(\mathbf{r})$ values at the CPs (3, −1) and (3, +1) for the keto-enol ring of tautomer **1A** found in the multipole refinement and

* To put the regions of the electron density accumulation in the DED and $\nabla^2\rho(\mathbf{r})$ maps into correspondence with one another, the $-\nabla^2\rho(\mathbf{r})$ function is presented in the sections.

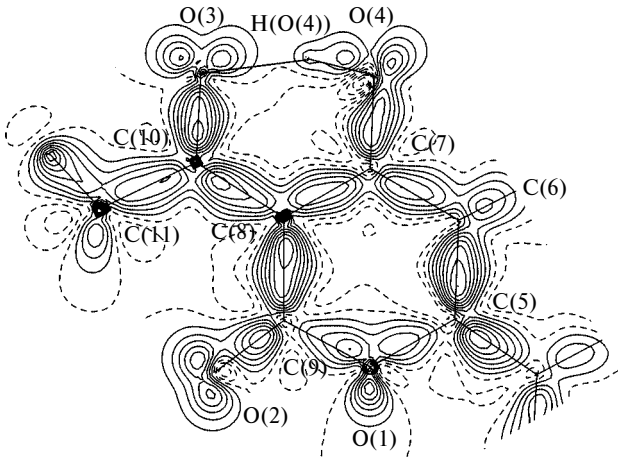

Fig. 5. Section of the static deformation electron density in the crystal of **1** at 100 K. The maps are contoured at intervals of 0.1 eÅ^{-3}. The negative contours are shown as dashed lines.

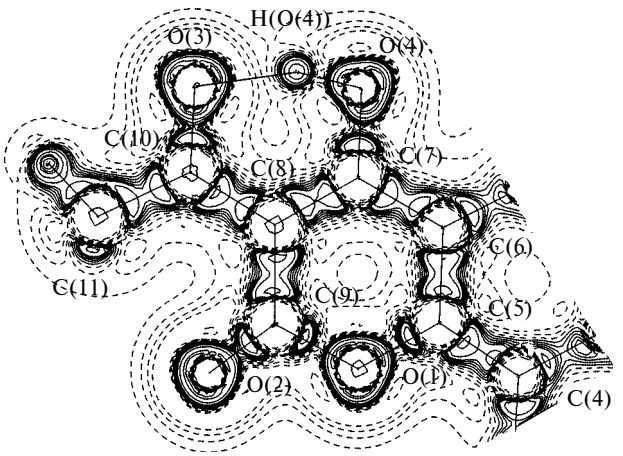

Fig. 6. Section of $-\nabla^2\rho(\mathbf{r})$ in the crystal of **1** at 100 K. The isolines are given in the logarithmic scale 2. The negative contours are shown as dashed lines.

determined from the B3LYP/6-31G(d,p) calculations are close. Earlier,[19] overestimation of the $\nabla^2\rho(\mathbf{r})$ values and bond ellipticities (ε) at the CPs (3, −1) for the O—C bonds in the crystal compared to the corresponding values obtained from the quantum-chemical calculations was attributed to the effect of the crystal field. Based on the local expression of the virial theorem (1), the similarity of the $\rho(\mathbf{r})$ and $\nabla^2\rho(\mathbf{r})$ values at the CPs (3, −1) in the region of the H-bond for tautomer **1A** in the crystal and in the gas phase suggests that the interatomic H(O(4))...O(3) bond in the crystal also belongs to the intermediate type of interactions.

The sign of $E(\mathbf{r})$ and, hence, the type of interactions can be directly estimated based on the X-ray diffraction data only if the density matrix $\rho(\mathbf{r},\mathbf{r}')$ is known.[9] Although such attempts have been undertaken in some studies (see, for example, Refs. 44 and 45), this problem still remains to be solved. However, it has been recently demonstrated[46] that an approximate description of the

density of the kinetic energy $G(\mathbf{r})$ (a.u.) as a function of $\rho(\mathbf{r})$ (a.u.) and $\nabla^2\rho(\mathbf{r})$ (a.u.) within the framework of the Thomas—Fermi theory

$$G(\mathbf{r}) = (3/10)(3\pi^2)^{2/3}\rho(\mathbf{r})^{5/3} + \nabla^2\rho(\mathbf{r})/6 \quad (2)$$

allows an estimation of $G(\mathbf{r})$ using the $\rho(\mathbf{r})$ and $\nabla^2\rho(\mathbf{r})$ values at the CPs (3, −1) determined from the multipole refinement. Application of this approximation to various systems demonstrated that the best agreement between the $G(\mathbf{r})$ values determined by Eq. (2) and those obtained directly from the density matrix is observed at large distances from the nucleus and, primarily, for closed-shell interactions (in this case, the discrepancy is ~5%; this value can exceed 20% for covalent bonds).[46]

According to the results of analysis of X—H...O contacts available in the literature (a total of 83 items), the above-mentioned approximation allows one not only to obtain semiquantititative estimates of the contributions to the local energy density, but also to associate these contributions with the energies of the H-bond (E_{HB}) and other weak specific interactions.[47,48] For instance, it was demonstrated that E_{HB} correlates with the density of the potential energy at the CP (3, −1):[47]

$$E_{HB}(\text{kJ mol}^{-1}) = 313.36V(\mathbf{r}) \text{ (a.u.)}. \quad (3)$$

This allows the use of high-resolution X-ray diffraction methods not only for elucidating the character of interatomic interactions but also for estimating their energies in crystals.[47—49] The dependence (3) agrees well with our results of analysis of the local energy contributions to the H-bonds in tautomers **1A** and **1B** according to which a change in the O—H distance leads to a change in $V(\mathbf{r})$, whereas $G(\mathbf{r})$ remians virtually unchanged (see Table 3).

As can be seen from Table 3, the estimation of $G(\mathbf{r})$ from Eq. (2) and subsequent calculations of $V(\mathbf{r})$ and $E(\mathbf{r})$ by Eq. (1) using the $G(\mathbf{r})$ and $\nabla^2\rho(\mathbf{r})$ values led to a very good agreement between the energy characteristics of the H(O(4))...O(3) hydrogen bond in the crystal and in the isolated molecule. This agreement suggests that the hydrogen bond in **1** both in the crystal and in the gas phase corresponds to the intermediate type of interatomic interactions.

The E_{HB} values for tautomer **1A** in the crystal and in the gas phase calculated by Eq. (3) are 26.3 and 33.8 kcal mol^{-1}, respectively. The high E_{HB} values for **1** agree well with the results of quantum-chemical calculations for **2**[19] and with the energies of intermolecular H-bonds in dimers of carboxylic acids.[50]

Since the assignment of particular intermolecular contacts to specific interactions in studies of the crystal packing depends essentially on the choice of the system of van der Waals radii, we performed the topological analysis of the electron density distribution function for the intermolecular contacts to establish which of the above-mentioned shortened contacts correspond to chemical interactions. We found that the CPs (3, −1) are localized in the regions of all the above-mentioned contacts (see Figs. 3 and 4), including both the interactions between the hydroxy groups and the stacking interactions of the H-bonded rings (Table 4). For the crystal of **1**, the $\rho(\mathbf{r})$ and $\nabla^2\rho(\mathbf{r})$ values at the CP (3, −1) corresponding to the C—H...O contacts agree well with the published data.[40,47—49] Calculations of $G(\mathbf{r})$, $V(\mathbf{r})$, and $E(\mathbf{r})$ by Eqs. (1) and (2) for all intermolecular interactions showed that the $E(\mathbf{r})$ values are positive in all cases. This means that all intermolecular contacts, unlike the intramolecular H-bonds in **1**, correspond to closed-shell interactions.

According to Poincare—Hopf's relationship,[42] bifurcated C—H...O bonds and stacking interactions must lead to the formation of intermolecular rings and polyhedra, respectively. As a result, additional CPs (3, +1) and (3, +3) should appear. Analysis of the CPs demonstrated that the above-mentioned relationship is fulfilled and the CPs (3, +1) and (3, +3) are localized both in the region of the bifurcated

Table 4. Principal topological characteristics of the intermolecular contacts (IMC) in the crystal of **1** based on the X-ray diffraction data collected at 100 K

IMC	$\rho(\mathbf{r})$ /eÅ^{-3}	$\nabla^2\rho(\mathbf{r})$ /eÅ^{-5}	$G(\mathbf{r})\cdot10^{-3}$	$V(\mathbf{r})\cdot10^{-3}$	$E(\mathbf{r})\cdot10^{-3}$	E* /kcal mol^{-1}
			a.u.			
		C—H...O contacts				
H(4)...O(1′)**[a]	0.048	0.76	6	−4	2	−1.4
H(4)...O(2′)**[a]	0.052	0.93	7	−5	2	−1.6
H(C(11))...O(3′)**[b]	0.034	0.76	6	−3	3	−1.1
		H(O(4))...O(4)..O(4′)H(O(4′)) contacts				
O(4)...O(4′)**[c]	0.052	1.09	9	−6	3	−1.8
		Stacking interaction				
C(7)...O(3′)**[d]	0.036	0.49	4	−3	1	−0.8
C(10)...O(4′)**[d]	0.036	0.51	4	−3	1	−0.8

* The energy E was estimated by Eq. (3).
** The atom was generated from the basis atom by the symmetry transformation:
[a] $-x, 1-y, 1-z$; [b] $x, -1+y, z$; [c] $1-x, 3-y, 1-z$; [d] $1-x, 2-y, 1-z$.

C—H...O bond and in the regions of the rings and polyhedra formed through stacking interactions. However, the type of the CP for the H-bonded C(7)O(3)O(4)C(10)C(7′′′)O(3′′′)O(4′′′)C(10′′′) polyhedron cannot be determined unambiguously because the $\rho(\mathbf{r})$ function and its curvature in the region of the expected CP (3, +3) corresponding to the polyhedron are small. As a result, the eigenvalues of the Hessian (λ_i) are close to zero.

With the aim of comparing these intermolecular interactions, we calculated their energies using Eq. (3). As can be seen from Table 4, the highest energy (~1.8 kcal mol^{-1}) is observed for unusual intermolecular interaction between the hydroxy groups and the lowest energy (0.81 kcal mol^{-1}) is observed for the C...O contact. However, the interaction between the H-bonded rings involves four C...O contacts and, consequently, the total energy of this interaction should be equal to ~3 kcal mol^{-1}, which is consistent with the estimate obtained previously[29] for the C=O...O=C interactions. Since the geometric characteristics of the intermolecular contacts, including the stacking interactions, in **1** and **2** are similar, it can be assumed that their energies are also comparable.

Therefore, the energies of the intermolecular contacts in the crystal of **1** (see Table 4) estimated from the results of B3LYP/6-31G(d,p) calculations are comparable with the height of the barrier to proton transfer (~2 kcal mol^{-1}). Taking into account a pronounced effect of the C—H...O contacts on both the molecular packing in crystals[51,52] and their conformations,[53] the contacts between the hydroxy groups and the π-systems of the H-bonded rings characterized by higher energies can have a more substantial effect on the height of the barrier to proton transfer and lead to the predominance of one of the tautomers. This fact precludes unambiguous transferability of the calculated barriers from the isolated molecule to the molecules in crystals even in the absence of strong H-bonds.

By and large, the quantum-chemical calculations of the proton transfer in 3-acetyl-4-hydroxycoumarin demonstrated that tautomers **1A** and **1B** have nearly equal energies, the energetically less favorable tautomer being characterized by the stronger intramolecular H-bond. Despite the low barriers to proton transfer (~2 kcal mol^{-1}) in **1**, no equalization of the bond lengths in the keto-enol ring and the formation of the 4e,3c-hydrogen bond are observed at 100 K. Analysis of the electron density distributions within the framework of the AM theory showed that the intramolecular H-bond both in the crystal and in the gas phase belongs to the intermediate type of interactions, which seems to be responsible for the low barrier and the high energy of the H-bond. The predominance of tautomer **1A** in the crystal is likely due to the presence of the C—H...O contacts and intermolecular interactions between the hydroxy groups and the π-systems of the H-bonded rings. The energies of these interactions estimated from the results of the electron density distribution study are comparable with the height of the barrier to proton transfer.

Experimental

The X-ray diffraction data were collected on a SMART 1000 CCD diffractometer using the ω scanning technique (the ω scan step was 0.3°; frames were exposed for 20 s). The data were processed with the use of the SAINT PLUS program package. The absorption correction was applied using the SADABS program. The principal crystallographic data and the characteristics of the refinement are given in Table 1. The structure was solved by the direct method and refined by the full-matrix least-squares method in the ansiotropic-isotropic approximation based on F^2. The positions of the H atoms were located from the difference electron density maps and were included in the refinement with isotropic thermal parameters. The central H(O(4)) atom was refined anisotropically. The calculations were carried out on a personal computer using the SHELXTL PLUS program package (version 5.0).

The multipole refinement of the data at 100 K was performed with the use of the XD program package.[53] For all nonhydrogen atoms, the coordinates, anisotropic thermal parameters, and the multipole parameters up to the octupole level ($l = 3$) were refined without symmetry restrictions. The H atoms were refined up to the dipole level ($l = 1$), except for the H(O(4)) atom for which the quadrupole populations were also refined ($l = 2$). Before the refinement, the C—H distances were normalized to the "ideal" value of 1.07 Å. The positions of the H atoms and their isotropic thermal parameters were not refined. The multipole refinement converged to $R = 0.0378$, $wR = 0.0424$, GOF = 1.2. The electron density maxima in the residual electron density maps ($\rho(\mathbf{r})_{exp} - \rho(\mathbf{r})_{multip}$) of **1** were no higher than 0.15 eÅ^{-3}; the maxima in the region of the O...H-bond were no higher than 0.06 eÅ^{-3}.

We thank N. L. Allinger (University of Georgia, Athens, USA) for help in performing quantum-chemical calculations and A. V. Manaev (the D. I. Mendeleev Russian University of Chemical Technology, Moscow, Russia) for providing 3-acetyl-4-hydroxycoumarin whose synthesis has been described previously.[11]

This work was financially supported by the Russian Foundation for Basic Research (Project Nos. 00-15-97359, 00-03-32807a, and 99-07-90133).

References

1. S. H. Bauer and C. F. Wilcox, *Chem. Phys. Lett.*, 1997, **279**, 122.
2. V. Barone and C. Adamo, *J. Chem. Phys.*, 1996, **105**, 11007.
3. J. A. Platts and K. E. Laidig, *J. Phys. Chem.*, 1996, **100**, 13455.
4. M. E. Tuckerman, D. Marx, M. L. Klein, and M. Parrinello, *Science*, 1997, **275**, 817.
5. J. Emsley, *Struct. Bonding*, 1984, **57**, 147.
6. *The Chemistry of Enols*, Ed. Z. Rappoport, Wiley, New York, 1990.
7. V. G. Tsirelson and R. P. Ozerov, *Electron Density and Bonding in Crystals: Principles, Theory, and X-ray Diffraction Experiments in Solid State Physics and Chemistry*, IOP Publishing Ltd, 1996.

8. R. F. W. Bader, *Atoms in Molecules. A Quantum Theory*, Clarendron Press, Oxford, 1990.
9. R. F. W. Bader, *J. Chem. Phys.*, 1998, **A102**, 7314.
10. R. F. W. Bader and H. Essen, *J. Chem. Phys.*, 1984, **80**, 1943.
11. V. F. Traven′, A. V. Manaev, O. B. Safronova, T. A. Chibisova, K. A. Lysenko, and M. Yu. Antipin, *Zh. Obshch. Khim.*, 2000, **70**, 853 [*Russ. J. Gen. Chem.*, 2000, **70** (Engl. Transl.)].
12. R. Boese, M. Yu. Antipin, D. Blaser, and K. A. Lyssenko, *J. Phys. Chem.*, 1998, **B102**, 8654.
13. F. L. Hirshfeld, *Acta Crystallogr., Sect. A*, **32**, 1976, 239.
14. J. E. Del Bene and I. Shavitt, in *Intermolecular Interactions: From van der Waals to Strongly-Bound Complexes*, Ed. S. Scheiner, Wiley, New York, 1997.
15. M. J. Frisch, G. W. Trucks, H. B. Schlegel, P. M. W. Gill, B. G. Johnson, M. A. Robb, J. R. Cheeseman, T. Keith, G. A. Petersson, J. A. Montgomery, K. Raghavachari, M. A. Al-Laham, V. G. Zakrzewski, J. V. Ortiz, J. B. Foresman, J. Cioslowski, B. B. Stefanov, A. Nanayakkara, M. Challacombe, C. Y. Peng, P. Y. Ayala, W. Chen, M. W. Wong, J. L. Andres, E. S. Replogle, R. Gomperts, R. L. Martin, D. J. Fox, J. S. Binkley, D. J. Defrees, J. Baker, J. P. Stewart, M. Head-Gordon, C. Gonzalez, and J. A. Pople, *GAUSSIAN-94W, Revision E. 2*, Gaussian, Inc., Pittsburgh (PA), 1995.
16. T. Maverick and K. N. Tueblood, *Thermal Motion Analysis Program THMA-11*, Zurich, 1987.
17. G. K. H. Madsen, B. B. Iversen, F. K. Larsen, M. Kapon, G. M. Reiser, and F. H. Herbstein, *J. Am. Chem. Soc.*, 1998, **120**, 10040.
18. F. H. Herbstein, B. B. Iversen, M. Kapon, F. K. Larsen, G. K. H. Madsen, and G. M. Reisner, *Acta Crystallogr., Sect. B*, 1999, **55**, 767.
19. B. Schiott, B. B. Iversen, G. K. H. Madsen, and T. C. Bruice, *J. Am. Chem. Soc.*, 1998, **120**, 12117.
20. P. Roversi, M. Barzaghi, F. Merati, and R. Destro, *Can. J. Chem.*, **74**, 1996, 1145.
21. G. Gilli, F. Bellucci, V. Ferretti, and V. Bertolasi, *J. Am. Chem. Soc.*, 1989, **111**, 1023.
22. P. Gilli, V. Bertolasi, V. Ferretti, and G. Gilli, *J. Am. Chem. Soc.*, 1994, **116**, 909.
23. V. Bertolasi, P. Gilli, V. Ferretti, and G. Gilli, *J. Am. Chem. Soc.*, 1991, **113**, 4917.
24. G. Gilli, V. Bertolasi, V. Ferretti, and P. Gilli, *Acta Crystallogr. Sect. B*, 1993, **49**, 564.
25. L. J. Altman and D. Laungani, *J. Am. Chem. Soc.*, 1978, **100**, 8264.
26. M. Basseti, G. Cerichelli, and B. Floris, *J. Chem. Res. (S).*, 1988, 236.
27. A. J. Vila, C. M. Lagier, and A. C. Olivieri, *J. Phys. Chem.*, 1991, **95**, 5069.
28. T. S. Kopteva and D. N. Shigorin, *Zh. Fiz. Khim.*, 1974, **48**, 532 [*Russ. J. Phys. Chem.*, 1974, **48**, 312 (Engl. Transl.)].
29. F. H. Allen, C. A. Baeelham, J. P. M. Lommerse, and P. R. Raithby, *Acta Crystallogr., Sect. B*, **54**, 1998, 320.
30. R. J. Boyd and S. C. Choi, *Chem. Phys. Lett.*, 1985, **120**, 80.
31. R. J. Boyd and S. C. Choi, *Chem. Phys. Lett.*, 1985, **129**, 62.
32. M. T. Carrol and R. F. W. Bader, *Mol. Phys.*, 1988, **65**, 695.
33. J. A. Platts, S. T. Howard, and B. R. F. Bracke, *J. Am. Chem. Soc.*, 1996, **118**, 2726.
34. J. A. Platts and K. E. Laidig, *J. Phys. Chem.*, 1996, **100**, 13455.
35. E. V. Valeev and H. F. Shaefer III, *J. Chem. Phys.*, 1998, **108**, 7199.
36. D. Madsen, C. Flensburg, and S. Larsen, *J. Phys. Chem.*, 1998, **A102**, 2177.
37. C. Flensburg, S. Larsen, and R. F. Stewart, *J. Phys. Chem.*, 1995, **99**, 10130.
38. M. Carcia-Viloca, A. Conzalez-Lafont, and J. M. Lluch, *J. Am. Chem. Soc.*, 1997, **119**, 1081.
39. M. Stebler and H.-B. Buergi, *J. Am. Chem. Soc.*, 1987, **109**, 1395.
40. P. R. Mallinson, K. Wozniak, G. T. Smith, and K. L. McCormack, *J. Am. Chem. Soc.*, 1997, **119**, 11502.
41. F. W. Biegler-König, R. F. W. Bader, and T.-H. Tang, *J. Comput. Chem.*, 1982, **3**, 317.
42. K. Collard and G. G. Hall, *Int. J. Quantum Chem.*, 1977, **12**, 623.
43. N. K. Hansen and P. Coppens, *Acta Crystallogr., Sect. A*, 1978, **34**, 909.
44. Yu. V. Aleksandrov, V. G. Tsirelson, I. M. Reznik, and R. P. Ozerov, *Phys. Status Solidi B,* 1989*,* **155**, 201.
45. K. Tanaka, *Acta Crystallogr.*, *Sect. B*, 1988, **45**, 1002.
46. Yu. A. Abramov, *Acta Crystallogr., Sect. A*, 1997, **53**, 264.
47. E. Espinosa, E. Mollins, and C. Lecomte, *Chem. Phys. Lett.*, 1998, **285**, 170.
48. P. Macchi, B. B. Iversen, A. Sironi, B. C. Chaukoumakos, and F. K. Larsen, *Angew. Chem., Int. Ed.*, 2000, **39**, 2719.
49. P. Coppens, Yu. Abramov, M. Carducci, B. Korjov, I. Novozhilova, C. Alhambra, and M. R. Pressprich, *J. Am. Chem. Soc.*, 1999, **121**, 2285.
50. G. A. Kumar and M. A. McAllister, *J. Am. Chem. Soc.*, 1998, **120**, 3159.
51. G. R. Deisraju, *Acc. Chem. Res.*, 1991, **24**, 290.
52. G. Müller, M. Lutz, and S. Harder, *Acta Crystallogr., Sect. B*, 1996, **52**, 1014.
53. T. Koritsansky, T. S. T. Howar, T. Richter, P. R. Mallinson, Z. Su, and N. K. Hansen, *XD, A Computer Program Package for Multipole Refinement and Analysis of Charge Densities from X-Ray Diffraction Data*, Free University of Berlin, Germany, 1995.

Received October 27, 2000